On the Microporous Nature of Transition Metal Nitroprussides

J. Balmaseda,[†] E. Reguera,*[,†] A. Gomez,[†] J. Roque,[†] C. Vazquez,[‡] and M. Autie[§]

Institute of Materials and Reagents, University of Havana, San Lazaro and L, 10400 Havana, Cuba, and Institute of Materials Research, UNAM, Mexico, and National Center for Scientific Research, Havana, Cuba

Received: December 10, 2002; In Final Form: July 14, 2003

Nitroprussides of divalent transition metals form a family of microporous molecular materials. Their properties in this sense depend on the transition metal cation involved and also on the preparative method, which determine their crystal structures. The stable phases of this family of materials belong to one of the following crystal structures: orthorhombic (*Pnma*) (Mn^{2+}, Fe^{2+}, Cu^{2+}, Zn^{2+}, and Cd^{2+}), cubic (*Fm*3*m*) (Co^{2+} and Ni^{2+}), and orthorhombic (*Amm*2) (Cu^{2+}). These materials are stable up to above 160 °C, while their dehydration takes place around 100 °C. On dehydration, *Amm*2 copper complex changes into a tetragonal (*I*4*mm*) phase. The microporous nature of these materials is discussed according to their crystal structure and correlating structural and adsorption data. The accessibility to the pore system was evaluated through adsorption of H_2O, CO_2, and N_2. Pores of both orthorhombic and cubic structures are accessible to H_2O and CO_2 in experiments carried out at 23 and 0 °C, respectively; however, they are inaccessible to N_2 at −196 °C. This behavior is discussed as related to the large polarizing power of the nitrosyl (NO) ligand which distorts the local environment of the iron atom and reduces the effective window cross section. The small pores of tetragonal copper nitroprusside were inaccessible to the adsorbates used.

1. Introduction

The studied materials are salts of the pentacyanonitrosylferrate(II) anion, $[Fe(CN)_5NO]^{2-}$, and of appropriate cations. Since only the N atoms of the CN ligands are able to link to the involved cation, in a tridimensional structure the NO ligand always remains unlinked at the O end. This leads to materials with a system of channels appropriate for small molecule separation.[1] The octahedral coordination sphere of the cation is commonly completed with coordinated water molecules. The microporous framework is usually filled with zeolitic waters which are hydrogen-bonded to the coordinated ones.[2−9] If both coordinated and zeolitic waters are removed, the available volume of these pores is significantly increased. The formation of an additional system of bigger and interconnected pores depends on the crystal structure adopted by the complex salt, and it is related to the occurrence of structural vacancies of both the complex anion and the cation (discussed below).

Nitroprussides are emerging as novel materials with promising applications in molecular communication and for storage information devices.[10−12] Their microporous nature opens the possibility of controlling the electronic structure and their physical properties through exchangeable species, e.g., filling their pores with appropriate molecular species, as has been observed in hexacyanides using ionic exchange.[13]

While hexacyanometalates have received certain attention as a prototype of microporous molecular materials,[1,14−18] the information available on pentacyanonitrosylferrates in this sense is very limited.[1] The crystal structure of nitroprussides has been resolved in the past decade.[2−9,19,20] This allows an evaluation of their behavior as microporous materials correlating structural and adsorption data. In this contribution, the microporous nature of Mn^{2+}, Fe^{2+}, Co^{2+}, Ni^{2+}, Cu^{2+}, Zn^{2+}, and Cd^{2+} nitroprussides is discussed from their crystal structure and H_2O, N_2, and CO_2 adsorption isotherms. That information is complemented with thermal and spectroscopic data.

2. Experimental Section

The studied materials were obtained mixing 0.01 M aqueous solutions of sodium nitroprusside and of a soluble salt of the above-mentioned cations (Mn^{2+}, Fe^{2+}, Co^{2+}, Ni^{2+}, Cu^{2+}, Zn^{2+}, and Cd^{2+}). The formed precipitates were then isolated by filtration, followed by successive washing to obtain a filtrate free of the starting anions and cations. The reagents used were analytical grade from Sigma and Merck. The resulting solids were air-dried and then stored in a desiccator over silica for aging. The nature and chemical composition of the obtained samples were established from infrared (IR) spectra, energy-dispersed X-ray spectroscopy (EDS), X-ray diffraction (XRD), thermogravimetry (TG), and Mössbauer data. The materials obtained in this manner were studied as fresh samples (air-dried at room temperature for a week) and after aging for five years.

IR spectra were collected using an FT-IR spectrophotometer (model Equinox 55 from Bruker) and samples diluted in KBr pressed disks. Parallel spectra were obtained from Nujol mulls in order to discard a possible mechano-chemical reaction of the analyte with the KBr matrix.[21] To obtain IR spectra of dehydrated samples a homemade glass cell with CaF_2 windows was used. EDS spectra were recorded with a Norand analytical unit coupled to a scanning electron microscope (JEOL model 35M). XRD patterns were run with Cu Kα radiation using a HZG4 diffractometer (from Jena). Some XRD patterns were also recorded using synchrotron radiation with $\lambda = 1.7477$ Å (at LNLS, Sao Paulo, Brazil). TG data were obtained using a TA instrument (model 1052) operated in the high-resolution mode and under a dried nitrogen flow. Mössbauer spectra were

* Corresponding author. Tel: +(537) 878 8956 to 878 8959, ext: 552. E-mail: edilso@ffuh.ff.oc.uh.cu.
[†] University of Havana.
[‡] Institute of Materials Research, UNAM.
[§] National Center for Scientific Research.

10.1021/jp027678g CCC: $25.00
Published on Web 09/23/2003

TABLE 1: Crystal Cell Parameters (*a*, *b* and *c*) and Space Group (SG) of the Studied Material (transition metal nitroprussides)

sample	*a*, Å	*b*, Å	*c*, Å	SG	ref
$Mn[Fe(CN)_5NO]\cdot 2H_2O$	14.322(7)	10.689(3)	7.671(2)	*Pnma*	8
$Fe[Fe(CN)_5NO]\cdot 2H_2O$	13.9864(19)	10.4768(12)	7.4372(9)	*Pnma*	19, 20
$Fe[Fe(CN)_5NO]\cdot 5H_2O$	10.330(2)			*Fm*3*m*	19, 20
$Co[Fe(CN)_5NO]\cdot 5H_2O$	10.257(1)			*Fm*3*m*	5
$Ni[Fe(CN)_5NO]\cdot 4H_2O$	10.168(1)			*Fm*3*m*	19, 20
$Cu[Fe(CN)_5NO]\cdot 2H_2O$	7.1947(3)	6.9840(3)	10.3519(3)	*Amm*2	20
$Cu[Fe(CN)_5NO]$	7.1179(1)		10.9308(2)	*I*4*mm*	20
$Zn[Fe(CN)_5NO]\cdot 2H_2O$	14.322(7)	10.689(3)	7.671(2)	*Pnma*	9
$Cd[Fe(CN)_5NO]\cdot {}_2H2O$	14.322(7)	10.689(3)	7.671(2)	*Pnma*	9

collected at room temperature on pressed disk samples in a constant acceleration spectrometer (MS 1101 from Mostech) operated in the transmission mode and using a $^{57}Co/Rh$ source. Mössbauer spectra of dehydrated samples were recorded using a glass cell similar to that used for IR spectroscopy but in this case with Mylar windows.

The N_2 adsorption isotherms were collected at −196 °C using Micromeritic equipment (model ASAP 2001). The adsorption of CO_2 was obtained by the volumetric method at 0 °C in a Pyrex glass equipment consisting of sample holder, dead volume, dose volume, and a manometer.[22] Water vapor adsorption isotherms were recorded at 23 °C in homemade equipment in which water is provided by evaporation from a calibrated capillary and the pressure is measured by an oil manometer. All the samples used in the adsorption experiments were previously evacuated for 4 h at 80 °C.

The adsorption data were evaluated according to the Dubinin−Astakhov (DA) model:[23]

$$n_{ad} = n_p \exp\{-[(RT/E_0)\ln(P_r^{-1})]^n\}$$

where n_{ad} represents the amount adsorbed at a relative pressure P_r, n_p is the limiting amount filling the micropores, E_0 is the characteristic energy, n is the heterogeneity parameter, R is the universal gas constant, and T is the Kelvin temperature. The model was fitted to experimental isotherms using a Levenberg−Marquardt minimization routine.[24] The starting values of the parameters to be fitted and the fitting region were estimated by plotting the experimental isotherm in Dubinin−Radushkevich coordinates ($n = 2$ in the above DA model). The pore volume estimation from H_2O and CO_2 isotherms was carried out, multiplying the respective n_p value by the molar volume in the liquid phase (18.06 mL/mol for H_2O and 42.9 mL/mol for CO_2[25]). The potential (A) involved in the adsorption process was calculated by[26,27] $A = E_0\{[\ln(1/\theta)]^{(1/n)}\}$, where θ is the fractional adsorption, and E_0 and n are derived fitting the experimental isotherms by the DA model.

Mössbauer spectra were fitted using a least-squares minimization algorithm and pseudo-Lorentzian line shape (implemented in the MossWinn program[28]) in order to obtain the values of isomer shift (δ), quadrupole splitting (Δ), line width (Γ), and relative area (A in %). The values of δ are reported relative to sodium nitroprusside.

The structural information used in the present study has been previously derived[9,20] from XRD powder patterns using the Rietveld method implemented in the *FullProf* program.[29]

3. Results and Discussion

On the Crystal Structure of the Studied Nitroprussides. This report includes a brief discussion on those structural features of transition metal nitroprussides relevant to understanding their behavior as microporous materials.

This family of materials shows a pronounced polymorphic character.[19,20] Slowly grown crystals of Mn^{2+}, Fe^{2+}, and Cd^{2+} nitroprussides result in monoclinic ($P2_1/n$) trihydrates, which preserve that structure while remaining within the mother liqueur.[3,4,19] For Zn^{2+} the obtained crystals are hexagonal (R3) trihydrates.[2] When these trihydrates, both monoclinic and hexagonal, are air-dried they lose a water molecule to form orthorhombic (*Pnma*) dihydrates,[19] which are the stable phases for these four cations. With the exception of the ferrous salt, the same orthorhombic (*Pnma*) dihydrates are obtained when the samples are prepared using the precipitation method.[19] Ferrous nitroprusside, when it is obtained as a precipitate, results in a cubic (*Fm*3*m*) pentahydrate, which on prolonged aging changess into the stable orthorhombic phase.[19,30] For Co^{2+} and Ni^{2+}, and for Fe^{2+} as non-aged precipitate, a cubic (*Fm*3*m*) phase is always observed with up to five water molecules per formula unit.[5,19] For Cu^{2+} three different phases can be obtained. Slowly grown crystals are orthorhombic (*Pnma*) stable dihydrates,[6] while precipitated samples also result in an orthorhombic dihydrate but with a different crystal structure (space group *Amm*2).[20] This last orthorhombic phase remains stable for at least five years of aging, and on heating it undergoes a reversible transformation to an anhydrous tetragonal (*I*4*mm*) phase.[20] On prolonged aging in humid air or after immersion in water, this anhydrous phase returns to its parent structure (orthorhombic *Amm*2 dihydrate). The orthorhombic (*Pnma*) dihydrate must be the most stable phase of copper nitroprusside since it is obtained through a slow diffusion process.[6] In Table 1 are collected the cell parameters of the studied materials.

All the stable phases of the studied family of materials belong to one of the following crystal structures: orthorhombic (*Pnma*) (Mn^{2+}, Fe^{2+}, Cu^{2+}, Zn^{2+}, and Cd^{2+}), cubic (*Fm*3*m*) (Co^{2+} and Ni^{2+}), and orthorhombic (*Amm*2) dihydrate (for Cu^{2+}). In all these structures the iron atom is coordinated to five C atoms of CN ligands and to the N atom of the NO group. The resulting octahedron, $[Fe(CN)_5NO]$, is distorted due to the large electron withdrawing effect (π-back-bonding) of the nitrosyl group (NO) with respect to the cyanide ligand. The NO group has a low-energy π^*-antibonding orbital which is partially populated by the t_{2g} electrons from the iron atom strengthening the ON−Fe bond. This causes the angle $N-Fe-C_{eq}$ (C_{eq} represents equatorial carbons) to be greater than the ideal value of 90°. The average $N-Fe-C_{eq}$ angle in the studied family of complexes is 95.7°. All the structural differences observed in the studied nitroprussides are related to the manner in which the ligands (CN and H_2O) are coordinating the outer metal.

In the orthorhombic (*Pnma*) phases the cation is coordinated by five CN ligands at the N end plus a water molecule. The second water molecule has a zeolitic character and is linked to the coordinated one through a hydrogen bond. Due to the different bond properties of the CN ligand and the water molecule, the resulting octahedron, $[M(NC)_5H_2O]$, is distorted.

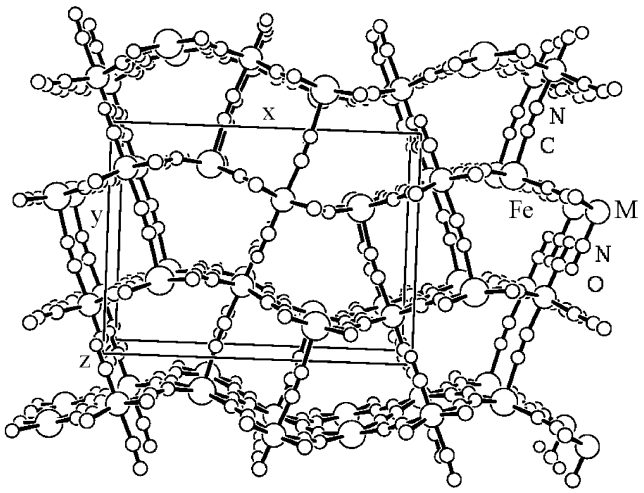

Figure 1. View along the *Z*-axis of the framework of orthorhombic (*Pnma*) nitroprussides, $M[Fe(CN)_6NO].xH_2O$ (M = Mn, Fe, Cu, Zn, Cd) illustrating the system of channels. Indicated is the unit cell of this structure.

On average, for the orthorhombic phases, the angle H_2O-M-N_{eq} (N_{eq} represents equatorial nitrogen) is 85.8°. Since in the orthorhombic structure the distorted octahedra, $[Fe(CN)_5NO]$ and $M(NC)_5(H_2O)$, are piled up maintaining antiparallel their NO and H_2O ligands, the resulting structure appears as a system of rippled sheets linked by CN ligands (Figure 1). In this framework there is a 3-dimensional channel system formed by the intersection of three different channels, two of them are in the [100] direction and have a prismatic shape with distorted trapezoidal and rectangular cross sections (Figure 1). In the following, these channels will be called "trapezoidal" and "rectangular", respectively. Coordinated water molecules are located within the trapezoidal channels, leaving a relatively small empty space close to the NO groups. In the monoclinic phase, that space is occupied by a second hydrogen-bonded water molecule.[3,4,19] Trapezoidal and rectangular channels are parallel and interconnected by lateral windows to form a large transversal cavity delimited by two walls of NO ligands. Once the coordinated water molecules are adsorbed, large cavities remain between NO ligands to accommodate the uncoordinated water molecules (Figure 1). These cavities are interconnected through relatively large windows to form sinusoidal channels.

In the orthorhombic (*Amm*2) structure, the copper atom is coordinated to four equatorial cyanides and two nonequivalent axial water molecules, $[Cu(NC)_4(H_2O)_2]$. The copper atom environment shows certain tetragonal distortion due to the Jahn−Teller effect. This is observed in its bond angle with the equatorial CN ligands, $N_{eq}-Cu-N'_{eq}$, which is 171°.[20] Since the axial cyanide ligand of $[Fe(CN)_5NO]$, which remains unlinked at N end, and the water molecules in $[Cu(NC)_4(H_2O)_2]$ adopt a parallel arrangement, the resulting structure appears as a sequence of rippled layers (Figure 2a). Within the crystal these layers are kept together by the Van der Waals forces. The loss of the two coordinated water molecules on dehydration leads to a structural transformation in order to increase the coordination number of the copper atom. Each layer shifts *a*/2 relative to a neighbor one, which allows the coordination of copper also to the axial cyanide. This results in a pyramidal (with a square base) coordination for the copper atom which is practically located on the base, $C_{eq}-Cu-C'_{eq} = 178°$ [20] (Figure 2b). The NO group remains unlinked but only at ca. 2.9 Å from the copper atom. This anhydrous tetragonal (*I*4*mm*) copper phase has a 3-dimensional system of communicated small pores formed by the intersection of two perpendicular channels. In the [100] direction there is a prism-shaped channel with rectangular cross section, which has a line of NO groups at the center of the largest rectangle side (Figure 2). The second channel is perpendicular to the first one and has a prismatic shape with square cross section (Figure 2).

The crystal structure of cubic nitroprussides can be resolved in the space group *Fm*3*m*, typical of Prussian blue analogues.[5,20] However, since the nitroprusside anion has C_{4v} symmetry where the axial NO ligand remains unbridged while in hexacyanide the symmetry is O_h, the analogy only concerns the average structure. In cubic nitroprussides, both inner and outer metals have 3/4 occupancy with three formula units per cell. This means that in the structure, cavities are formed by vacancies of both metals. A vacancy of the inner metal and its environment of ligands leads to a cavity with a diameter of ca. 8 Å. In this cubic array of $[Fe(CN)_5NO]$ blocks, the vacancy of the outer metal is related to the existence of unbridged NO ligands at the O end. In the *Fm*3*m* structure, six molecular blocks $[Fe(CN)_5NO]$ are arranged in such a way that their six unbridged NO groups are oriented toward the center of a cube forming a second cavity (the nitrosyl bound cage) with a diameter of ca. 5 Å (Figure 3). The first cavity (the water bound cage) is usually filled with removable water molecules, coordinated and uncoordinated (zeolitic), up to 15 molecules per unit cell. The nitrosyl bound cage is free of water, suggesting that the NO group behaves as a hydrophobic center.

Mössbauer and IR spectroscopies also provide structural information on the studied materials. Mössbauer parameters (δ and Δ) of iron in the structural unit $[Fe(CN)_5NO]$ are practically independent of the outer metal and of the crystal structure adopted by a given composition (Table 2). The strongly bonded CN and NO ligands effectively shield the iron atom from changes in the outer environment. Due to that strong interaction, the iron atom adopts a low spin electronic configuration, as can be inferred from the value of δ.[30,31] The nitrosyl group has a low-energy π^*-antibonding orbital at its N end which abstracts electrons from the iron d_{xz} and d_{yz} orbitals creating a pronounced charge asymmetry around the iron atom which is observed as a large quadrupole splitting value (∼1.80−1.95 mm/s) (Table 2). This strong π-back-bonding of the NO group leads to a significant reduction of the 3d electron shielding effect on the s-electron density at the iron nucleus, which explains the extremely low values of isomer shift in nitroprussides (Table 2).

According to the Mössbauer spectra of cubic ferrous nitroprusside, in the cubic structure there prevails a certain disorder which favors the *Fm*3*m* structure, on average. In Mössbauer spectra of the cubic phase, there appear three quadrupole doublets (Figure 4) of high spin Fe(2+) which correspond to three different structural sites for the outer metal in the cubic structure, in a relative population of 72:18:10 (Table 2). According to the Mössbauer parameters (δ and Δ), the most populated site (72%) has a local composition similar to that found in the orthorhombic complex, $[Fe(NC)_5H_2O]$. The weakest doublet (10%) has the smaller value of Δ and consequently must correspond to a highly symmetric structural site, tentatively assigned to iron atoms coordinated to six CN ligands at the N end, $[Fe(NC)_6]$. To the doublet of intermediate population (18%) corresponds the higher Δ value and a very asymmetric environment for iron, e.g., $[Fe(NC)_4(H_2O)_2]$. This assignment of doublets to local environments is in agreement with the observed positive correlation between δ and Δ (Table 2 and Figure 5). The variation of isomer shift in high-spin iron complexes is

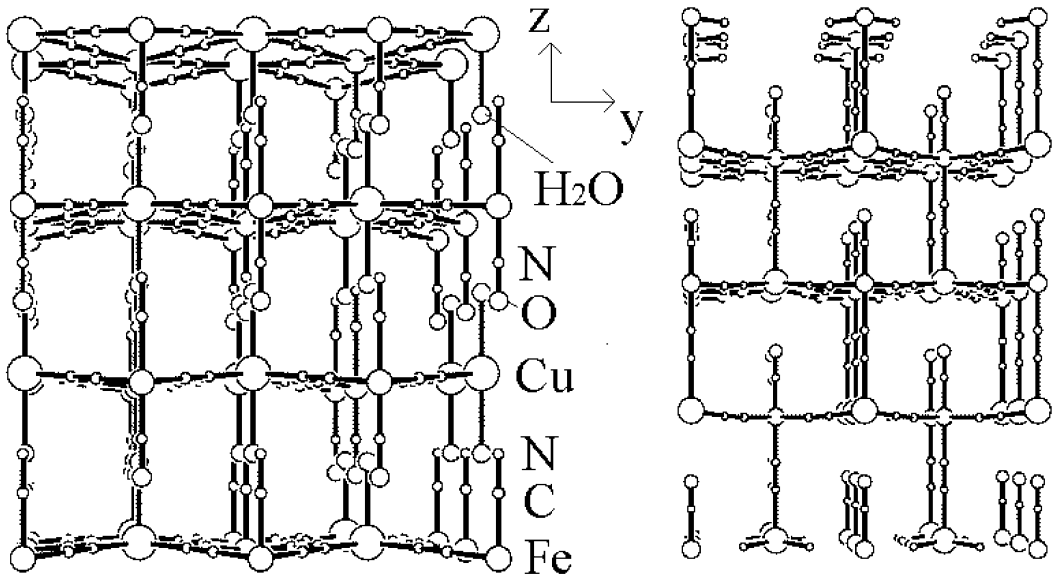

Figure 2. Atomic packing for copper nitroprusside: (a) layered structure in orthorhombic (*Amm*2) dihydrate; (b) anhydrous tetragonal (*I*4*mm*) phase illustrating the existence of a small channel around the NO group. The Jahn−Teller distortion of the copper atom environment can be observed in both structures.

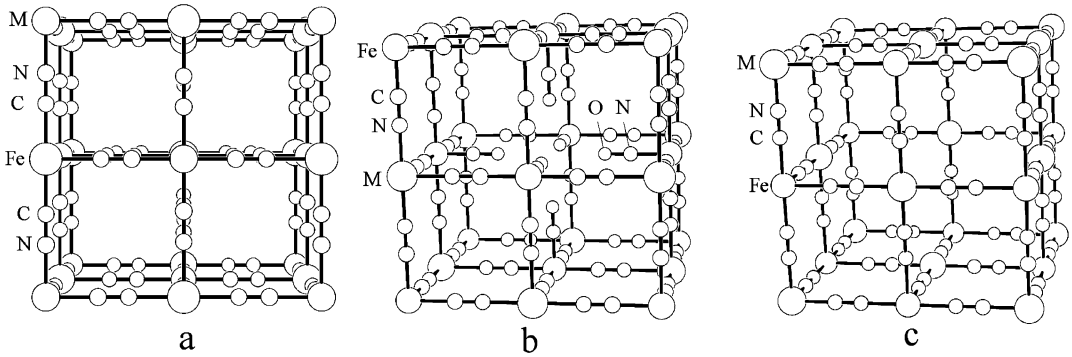

Figure 3. Pores (cages) in cubic (*Fm*3*m*) nitroprussides, M[Fe(CN)$_5$NO] (M = Fe, Co, Ni): (a) small cubic cage; (b) the nitrosyl bound cage; (c) a large pore created by a vacancy of the [Fe(CN)$_5$NO] structural unit. In these cubic materials the largest pores are interconnected through the small cubic ones.

mainly due to the degree of occupation of the 4s orbital of iron from the ligands electrons.[31] An increase in the s-electron density at the iron nucleus produces a decrease in the value of δ[31]. The CN ligand is a better σ-donor than the water molecule, and consequently, the substitution of CN ligands by water molecules in the iron coordination sphere not only reduces the symmetry of its environment increasing Δ but also the value of δ through a reduction in the 4s electron density at the iron nucleus. This explains the observed positive correlation of δ vs Δ, which supports the above-discussed assignment of Mössbauer subspectra to structural sites for the iron atom.

IR spectra contain information regarding both the structural units and the adsorbed species. Weakly bonded waters have broad ν(O−H) adsorption bands in the 3250−3400 cm^{-1} region, while for the coordinated ones these bands are very narrow.[19] In the orthorhombic (*Amm*2) phase of copper nitroprusside, where the two waters are coordinated, the Jahn−Teller distortion of the copper environment can be observed as two well-defined δ(H−O−H) vibrations corresponding to two nonequivalent water molecules (Figure 6). In that phase, the unlinked cyanide ligand appears with a ν(CN) absorption ca. 47 cm^{-1} below the band corresponding to the linked ones. On dehydration (and phase transformation), that low-frequency ν(CN) absorption disappears since now all the cyanide ligands have become linked (Figure 6).

Dehydration Process and Thermal Stability. Orthorhombic (*Pnma*) nitroprussides have TG curves with the first weight loss in the 40−100 °C region (Figure 7a). Then the sample weight remains stable up to above 160 °C, where the decomposition process begins with a weight loss corresponding to the evolution of the NO and a CN ligands. The first weight loss, up to 100 °C, corresponds to the evolution of two water molecules per formula unit. In this region, the TG curves show an intermediate inflection point, revealed by the corresponding derivative curve (Figure 7a). That inflection suggests that first the hydrogen-bonded water molecule (zeolitic) is evolved and then the tighter one (coordinated)(Figure 7a). This is effectively confirmed in the water vapor adsorption experiments (discussed below). In the TG curve of orthorhombic (*Amm*2) copper nitroprusside, that inflection is not present (Figure 7b) since the two waters are coordinated and their small structural difference, related to the Jahn−Teller effect of copper(II) ion, cannot be detected using this technique. Its derivative curve shows a single peak (Figure 7b). The TG curves of cubic nitroprussides are very complex, particularly in the region corresponding to the dehydration process, up to 100 °C. In the corresponding derivative curve, several inflections are observed (Figure 7c). It seems the evolution of the zeolitic waters takes place in several steps (or as a continuous process), which cannot be resolved, even using the high-resolution TG mode. The loss of zeolitic

TABLE 2: Mössbauer Parameters at Room Temperature of the Studied Materials, as Hydrated Dehydrated Samples[a] (For the ferrous complex also the parameters of the monoclinic phase are included.)

sample	δ[b], mm/s	Δ, mm/s	Γ, mm/s	assignment[c]
$Mn[Fe(CN)_5NO]\cdot 2H_2O$	0.00	1.86	0.25	Fe^{II}
$Mn[Fe(CN)_5NO]$	0.00	1.84	0.36	Fe^{II}
$Fe[Fe(CN)_5NO]\cdot 3H_2O$	0.00	1.84	0.26	Fe^{II}
(monoclinic, $P2_1/n$)	1.40	2.04	0.31	$Fe^{2+}N_5(H_2O)$
$Fe[Fe(CN)_5NO]\cdot 2H_2O$	−0.01	1.86	0.24	Fe^{II}
(orthorhombic, *Pnma*)	1.39	1.22	0.32	$Fe^{2+}N_5(H_2O)$
$Fe[Fe(CN)_5NO]\cdot 5H_2O$	0.03	1.90	0.26	Fe^{II}
(cubic, *Fm*3*m*)	1.37	1.41	0.36	$Fe^{2+}N_5(H_2O)$
	1.40	2.58	0.33	$Fe^{2+}N_4(H_2O)_2$
	1.32	0.47	0.24	$Fe^{2+}N_6$
$Fe[Fe(CN)_5NO]$	−0.04	1.93	0.28	Fe^{II}
(*Fm*3*m*, dehydrated)	1.36	1.32	0.61	$Fe^{2+}N_5$
	0.98	1.50	0.43	$Fe^{2+}N_4$
	1.28	0.47	0.25	$Fe^{2+}N_6$
$Co[Fe(CN)_5NO]\cdot 5H_2O$	−0.02	1.92	0.25	Fe^{II}
$Co[Fe(CN)_5NO]$	−0.02	1.91	0.29	Fe^{II}
$Ni[Fe(CN)_5NO]\cdot 4H_2O$	0.02	1.93	0.27	Fe^{II}
$Ni[Fe(CN)_5NO]$	−0.02	1.94	0.29	Fe^{II}
$Cu[Fe(CN)_5NO]\cdot 2H_2O$	0.01	1.64	0.23	Fe^{II}
$Cu[Fe(CN)_5NO]$	−0.01	1.80	0.23	Fe^{II}
$Zn[Fe(CN)_5NO]\cdot 2H_2O$	0.00	1.87	0.24	Fe^{II}
$Zn[Fe(CN)_5NO]$	0.01	1.86	0.25	Fe^{II}
$Cd[Fe(CN)_5NO]\cdot 2H_2O$	0.01	1.86	0.23	Fe^{II}
$Cd[Fe(CN)_5NO]$	0.01	1.82	0.33	Fe^{II}

[a] Error in δ, Δ, and Γ are smaller than 0.01 mm/s. [b] Isomer shift values are reported relative to sodium nitroprusside. [c] Fe^{II}, low-spin ferrous iron; Fe^{2+}, high-spin ferrous iron.

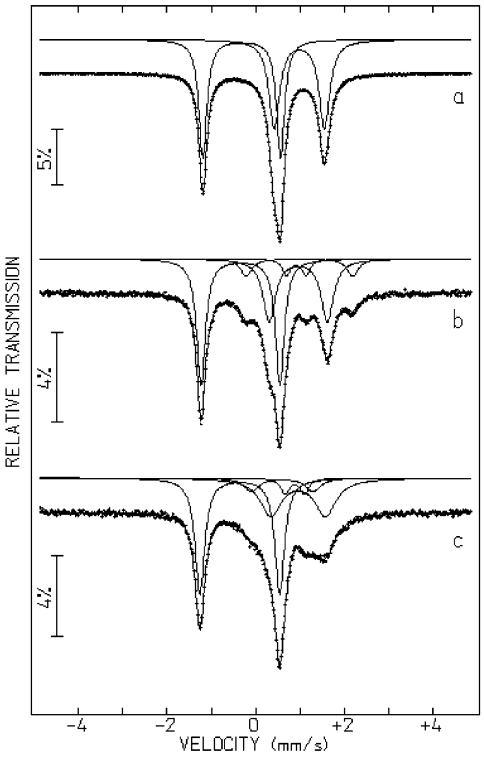

Figure 4. Mössbauer spectra at room temperature of ferrous nitroprusside: (a) orthorhombic (*Pnma*) dihydrate; (b) cubic (*Fm*3*m*) pentahydrate; (c) similar to (b) but dehydrated in a vacuum at 100 °C. On dehydration, only the environment of the external metal is altered.

water begins as soon as the sample is heated, and even in nonheated samples if they are maintained under a dry nitrogen flow. According to the weight loss, Co^{2+} and Fe^{2+} (*Fm*3*m*) nitroprussides are pentahydrates while the Ni^{2+} one is a

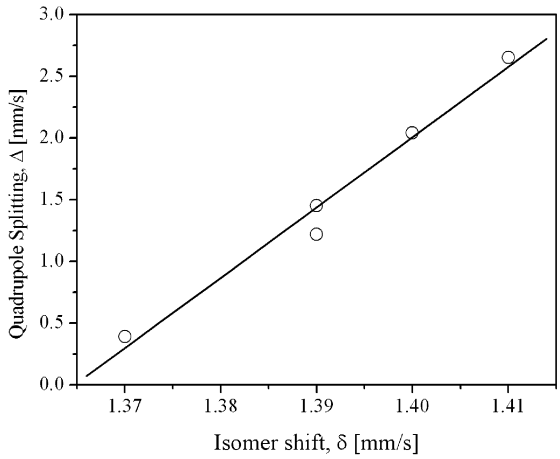

Figure 5. Correlation of quadrupole splitting (Δ) and isomer shift (δ) for the outer cation (Fe^{2+}) in ferrous nitroprussides.

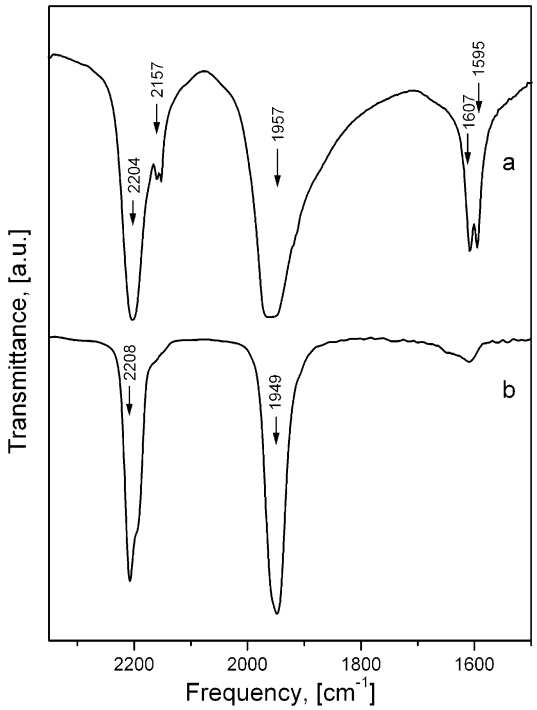

Figure 6. IR spectra (2350−1000 cm^{-1} region) of copper nitroprusside: (a) orthorhombic (*Amm*2) dihydrate; (b) anhydrous tetragonal (*I*4*mm*) phase. In the hydrate phase a cyanide ligand remains unlinked and the coordinated water molecules are not equivalent due to the Jahn−Teller distortion of the Cu(II) environment (see Figure 2).

tetrahydrate. As in the orthorhombic phases, cubic nitroprussides are also stable on heating to above 160 °C.

The Mössbauer spectrum is an excellent sensor of the local changes that take place on the dehydration (activation) process. No significant changes are observed in the values of δ and Δ for the iron cation within the complex anion on water removal (Figure 4 and Table 2). This means that while the temperature remains within the stability range for these materials (on average, below 160 °C), the $[Fe(CN)_5NO]$ structural unit is not affected by the heating process. The exception in this behavior is observed for orthorhombic (*Amm*2) copper nitroprusside, which undergoes a phase transformation on dehydration. In its anhydrous phase the pentacoordinated copper atom has a physical interaction with a neighboring oxygen atom of a nitrosyl group (Figure 2). The Cu−ON distance, ca. 2.9 Å, is insufficient for a chemical interaction but sufficient for a physical one. The

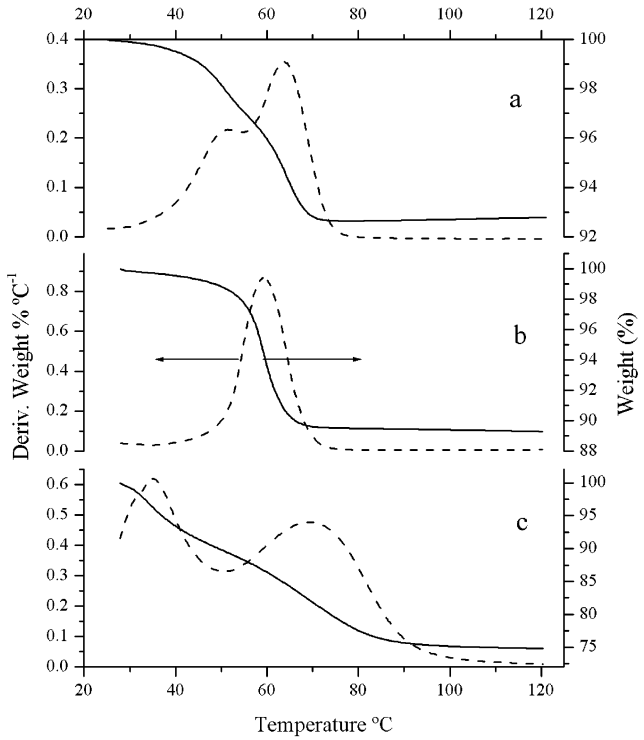

Figure 7. TG curves and their derivatives (dehydration region) of (a) cadmium nitroprusside; (b) copper nitroprusside (*Amm*2) dihydrate; (c) ferrous nitroprusside (a nonaged precipitate). The behavior of Cd^{2+} (a) and Fe^{2+} (c) nitroprussides on heating are characteristic of the orthorhombic (*Pnma*) and cubic (*Fm*3*m*) phases.

positively charged copper atom polarizes the NO electron cloud from the oxygen side. This favors an increase of the NO π-back-bonding interaction with the iron atom, resulting in a higher asymmetry of the iron charge environment, which is detected as a slightly higher value of Δ, when compared to the value of this parameter in the parent dihydrate (Table 2). That increase in the π-back-bonding interaction is also detected as a decrease in the value of δ (Table 2).

On dehydration, the outer metal in orthorhombic (*Pnma*) nitroprussides loses the coordinated water and becomes pentacoordinated. In this new configuration, the metal could move toward the center of the resulting pyramid of ligands in such a way that this site in ferrous nitroprusside reduces its Δ value (Table 2). The same behavior is observed in the analogous site of the cubic ferrous phase (Figure 4 and Table 2). Perhaps the most significant change in the Mössbauer parameters of ferrous cubic nitroprusside on dehydration is observed for the $Fe(NC)_4(H_2O)_2$ site. According to its large Δ value (Table 2), the two coordinated water molecules must be disposed as neighboring ligands ($H_2O-Fe-OH_2$ angle $\sim 90°$). The removal of these two water molecules leads to tetrahedral coordination for the iron atom. In that case, a drastic reduction in the value of Δ would be expected, which is effectively observed on the dehydration process of this complex (Figure 4 and Table 2).

IR spectra can also be used to study the dehydration process and thermal stability of the studied materials. On dehydration, the IR water absorption bands ν(OH) and δ(H−O−H) disappear, while the skeletal vibrations ν(CN), ν(NO), ν(Fe−C), and δ(Fe−C≡N) are preserved with only small shifts relative to their initial absorption frequencies. The exception in this behavior is the orthorhombic *Amm*2 phase of copper nitroprusside where, on dehydration and related phase transformation, the ν(CN) band corresponding to the unlinked cyanide disappears (Figure 6).

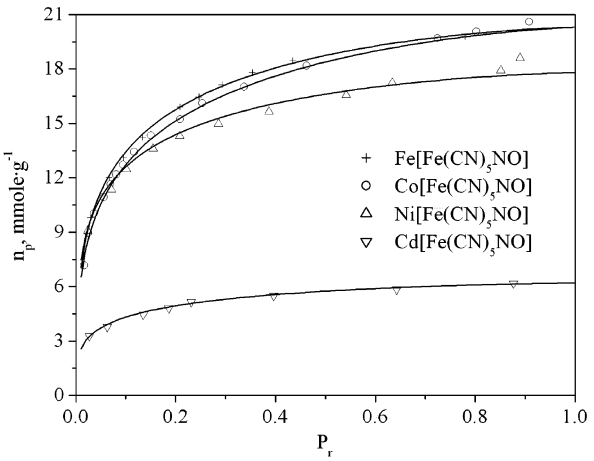

Figure 8. Isotherms of water vapor adsorption at 23 °C in Cd^{2+}, Fe^{2+}, Co^{2+}, and Ni^{2+} nitroprussides. These isotherms are in correspondence with the microporous structure of these materials.

The decomposition process in these materials begins with the loss of the NO group, which can be monitored by the change in intensity of the ν(NO) vibration in the corresponding IR spectra.

Adsorption Isotherms. According to the above-discussed structural features of the studied materials, the adsorption study can be limited to some compositions representative of *Fm*3*m*, *Pnma*, and *I*4*mm* structures. Therefore, the adsorption study was mainly carried out on Co^{2+}, Cd^{2+}, and Cu^{2+} nitroprussides, which are representative of these space groups. However, considering that the largest pore size corresponds to the cubic structure, in the water adsorption study, Ni^{2+} and Fe^{2+} (cubic) nitroprussides were also considered. The Dubinin theory of pore filling, usually applied to study the adsorption process in carbons and zeolites,[25,27,32] which has also proved to be useful in the evaluation of hexacyanometalates[14,18] as microporous materials, now will be used in this study on the microporous nature of transition metal nitroprussides.

Figure 8 shows the water adsorption isotherms in Cd^{2+}, Fe^{2+}, Co^{2+}, and Ni^{2+} nitroprussides. These isotherms are characteristic of microporous materials. At relatively low relative pressures, the adsorption of a large amount of water molecules takes place, particularly those water molecules that would be coordinated to the outer metal. Their absorption ends at equilibrium pressures below the minimum detectable by the equipment used (0.1 Torr). Therefore, the recorded isotherms contain information about the whole sample adsorption capacity but fail to shed light on the guest−host interaction in the adsorption domain of coordinated waters. The coordinated water is strongly bonded through its oxygen atom to the outer metal. The polarization of the oxygen electrons by the metal increases the ability of the water hydrogen atoms to form hydrogen bonds, for instance, with two water molecules. This is observed in trihydrated Mn^{2+}, Fe^{2+}, and Cd^{2+} nitroprussides (monoclinic $P2_1/n$). This means that the adsorption of the coordinated waters leads to the appearance of new adsorption sites.

The rehydration of the anhydrous Cu^{2+} complex (tetragonal) takes weeks, even in an atmosphere saturated in water vapor. This slow kinetic is related to the phase transformation from the anhydrous (tetragonal) phase to form the *Amm*2 orthorhombic dihydrate. As already mentioned, in nitroprussides the most stable water molecule is found bonded to the outer metal. In the anhydrous phase the copper atom is pentacoordinated, but its available coordination site remains shielded by a neighboring NO group. It seems the NO group is unable to stabilize adsorbed

TABLE 3: Results Obtained Fitting the H_2O, N_2, and CO_2 Adsorption Isotherms on Activated M[Fe(CN)$_5$NO] Samples through a Dubinin Model (n_p, the limiting amount adsorbed filling the micropores; E_0, characteristic energy; n, heterogeneity parameter; V_p, pore volume; x, number of adsorbed molecules per formula unit)

complex	adsorbate	n_p, mmol/g	E_0, J mol^{-1}	n	V_{pore}, cm^3/g	x
Cd[Fe(CN)$_5$NO]	H_2O	6.2 ± 0.2	12393 ± 539	1.3 ± 0.1	0.111 ± 0.003	2.00 ± 0.05
	CO_2	2.6 ± 0.1	14370 ± 237	3.3 ± 0.2	0.111 ± 0.004	0.85 ± 0.03
	N_2	3.3 ± 0.2	17089 ± 985	2.9 ± 0.3	0.115 ± 0.008	1.08 ± 0.07
Co[Fe(CN)$_5$NO]	H_2O	20.3 ± 0.2	10242 ± 134	1.29 ± 0.05	0.367 ± 0.003	5.58 ± 0.05
	CO_2	8.9 ± 2.6	6929 ± 1147	1.6 ± 0.2	0.38 ± 0.11	2.4 ± 0.7
	N_2	10.4 ± 0.6	8240 ± 138	1.34 ± 0.07	0.36 ± 0.02	2.9 ± 0.2
Fe[Fe(CN)$_5$NO]	H_2O	20.3 ± 0.2	10812 ± 155	1.37 ± 0.05	0.367 ± 0.003	5.53 ± 0.05
Ni[Fe(CN)$_5$NO]	H_2O	17.8 ± 0.3	12552 ± 263	1.34 ± 0.08	0.322 ± 0.005	4.90 ± 0.08

waters in its environment through hydrogen-bonding interactions. On air-drying, monoclinic ($P2_1/n$) trihydrates easily lose the zeolitic water molecules that are in the neighborhood of the NO groups.[19] Likewise, the nitrosyl-bound cage in cubic nitroprussides is free of water molecules.[5] The oxygen atom of the NO group is engaged in a triple bond with the nitrogen one, which reduces its ability to form a hydrogen bond with a water molecule.

According to the limiting amount filling the micropores (n_p), cadmium nitroprusside (orthorhombic *Pnma*) adsorbs two water molecules per formula unit (Table 3), which is in agreement with the TG results. The first adsorbed water is located in the coordination sphere of the Cd^{2+} atom, and then it serves to adsorb a second water through a hydrogen-bond interaction. The adsorption of this second water is also an energetic process due to the high ability of the coordinated water to form a hydrogen bond. The relatively large energy involved in that process leads to a high adsorption kinetic. The observed adsorption isotherm practically corresponds to the saturation region (Figure 8). The pore volume, estimated from n_p,was 0.111 cm^3 g^{-1}, which is slightly smaller than that reported for some zeolites (mordenite: 0.165 cm^3 g^{-1}; clinoptilolite: 0.198 cm^3 g^{-1})[33] and cadmium ferricyanide (0.184 cm^3 g^{-1}).[18] The value of the heterogeneity parameter (n), derived from the fitting of the DA model, is 1.3. This relatively small value of n is in correspondence with the broad peak observed in the TG curve for the loss of the weakly bonded water in this material (Figure 7a). It seems this adsorbent−adsorbate system behaves as a solid solution. The dehydration and rehydration processes take place with a broad distribution of energy. A similar behavior was also observed in cubic nitroprussides (discussed below).

Cubic nitroprussides (complexes of Fe^{2+}, Co^{2+}, and Ni^{2+}) have similar water adsorption isotherms revealing the adsorption of a large amount of hydrogen-bonded water (Figure 8). The first points of these curves correspond to the adsorption of the first hydrogen-bonded water molecule. In this region the adsorbed amount rapidly increases due to that relatively strong interaction. The following water molecule to be adsorbed also forms a hydrogen bond with the coordinated one. From this point, the remaining molecules are sited, forming a weaker hydrogen bond with these two first adsorbed waters or between themselves to form a water cluster. The energy liberated in the pore filling progressively decreases which leads to a reduction in the kinetic of the adsorption process. According to the estimated n_p values (Table 3), cubic nitroprussides adsorb up to four hydrogen-bonded water molecules per formula unit, sufficient to form a water cluster, which is in correspondence with the TG results, and also with the reported crystal structure for the Co^{2+} complex. The Ni^{2+} complex only adsorbs three hydrogen-bonded water molecules per formula unit. This was attributed to the large polarizing power of this cation[34] which leads to a significant local distortion of its environment, reducing the available volume of the largest pores. These pores are delimited by six nickel atoms and their environment of ligands. This effect is also observed as a cell contraction. The smallest cell edge in cubic nitroprussides is observed for the Ni^{2+} complex (Table 1). The pore volume estimated for cubic nitroprussides was approximately three times that found for the orthorhombic structure (Table 3). According to the above-discussed structures of transition metal nitroprussides, this was an expected result.

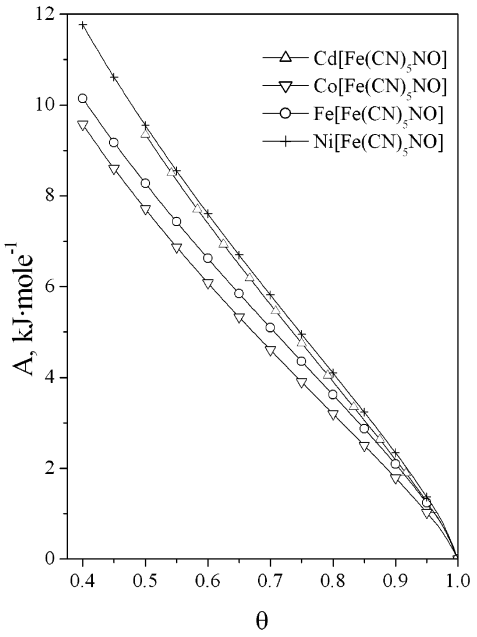

Figure 9. Dependence of the adsorption potential (A) on the fractional adsorption (θ) derived from the water isotherms in Cd^{2+}, Fe^{2+}, Co^{2+}, and Ni^{2+} nitroprussides.

The adsorption potential (A) estimated from water adsorption isotherms, using the fitted parameters n and E_0, falls in the range 0−16000 and 0−12000 J/mol, for the orthorhombic and cubic phases, respectively (Figure 9). Since the contribution from the hydrogen-bonding interactions falls in the range 0−10000 J/mol,[35] the difference, 6000 (and 2000) J/mol, results from dipole−dipole interactions between adsorbed water molecules and also probably from a minor contribution of Van der Waals forces. The adsorption potential curves for Fe^{2+} and Co^{2+} nitroprussides are very similar with practically the same A values in all the range of fractional adsorption (θ). The curves corresponding to the Ni^{2+} and Cd^{2+} complexes practically overlap, indicating that in these compositions the water molecules are adsorbed, on average, with practically the same energy. As already mentioned, the amount of hydrogen-bonded water molecules in the Ni^{2+} is insufficient to form water clusters. The hydrogen-bonding interactions are dominated by the coordinated water which is linked to a highly polarizing cation. This explains the relatively large A values for this complex.

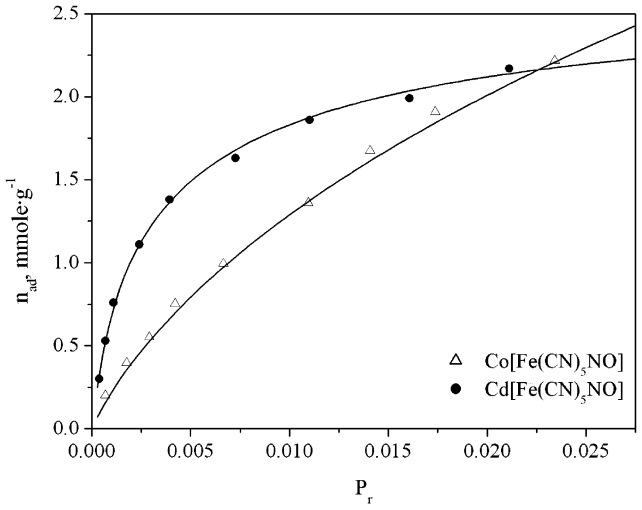

Figure 10. CO_2 adsorption isotherms at 0 °C in Cd^{2+} and Co^{2+} nitroprussides. These isotherms suggest that CO_2 really fills the microporous systems of these materials.

Figure 10 shows the adsorption isotherms of CO_2 at 0 °C in Cd^{2+} and Co^{2+} nitroprussides. In Table 3 are included the values of those parameters derived from a fitting of these isotherms with the DA model. The maximum adsorption in the orthorhombic structure corresponds to 0.85 CO_2 molecules per formula unit. The fast increase in the adsorption of CO_2 in the Cd^{2+} complex at relatively low pressures suggests a strong guest−host interaction which facilitates the adsorption process. This was interpreted as a combined effect due to the surface electric field gradient and the small pore size. It seems the pore size of the orthorhombic guest structure is close to the kinetic diameter of the CO_2 molecule (3.45 Å). This confinement favors a strong Van der Waals interaction. The electric field gradient at the pores is able to interact with the electric quadrupole moment of the CO_2 molecule; this interaction is also favored in a confined system since it has an R^{-4} dependence where R is the distance between the interacting species, in this case the CO_2 molecule and the material surface. Probably the main contribution to the adsorption potential within these pores is due to this last interaction, and suggests the pore filling in cubic nitroprussides (discussed below). Orthorhombic nitroprussides have 4 formula units per cell which means the adsorption of 3.4 CO_2 molecules in the unit cell. According to Figure 1 the unit cell of this structure contains 4 trapezoidal channels. This suggests the accommodation of CO_2 molecules within these channels forming linear chains. The CO_2 molecule has an ellipsoidal shape which facilitates such an orientation. This could explain the high value of the heterogeneity parameter n estimated from the adsorption of CO_2 in the Cd^{2+} complex. A large n value corresponds to a narrow distribution of the adsorption energy.

An analogous reasoning for Co^{2+} nitroprusside leads to 7.2 CO_2 molecules adsorbed per unit cell. According to the molar volume of CO_2 (42.9 mL/mol), the adsorption of a CO_2 molecule requires a volume of 71 Å^3. The largest pore in these nitroprussides has an estimated diameter of ca. 8 Å, and its volume (∼512 Å^3) would be sufficient to accommodate these 7.2 CO_2 molecules. However, this structure only has 25% of vacant outer metal sites per unit cell, which are responsible for the largest pore formation. This means that CO_2 molecules are also filling the small pores of this structure. The obtained value of n (heterogeneity parameter) for Co^{2+} nitroprusside is 1.6, which corresponds to a broad distribution of the adsorption energy. This could be interpreted as the existence of adsorption

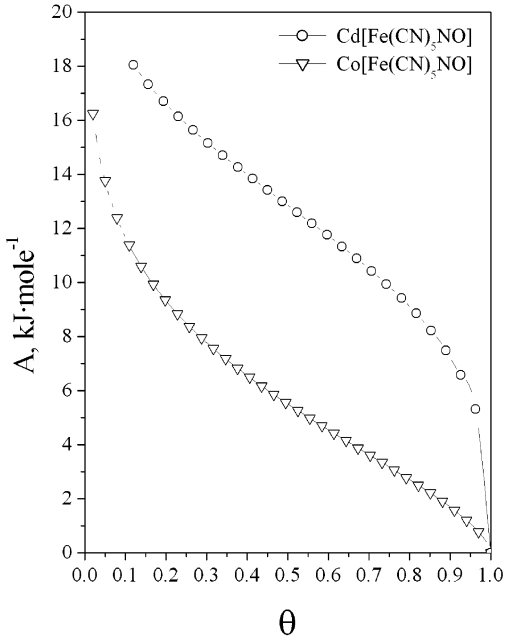

Figure 11. Dependence of the adsorption potential (A) on the fractional adsorption (θ) derived from the CO_2 isotherms in Cd^{2+}, Fe^{2+}, Co^{2+}, and Ni^{2+} nitroprussides.

sites with quite different adsorption potentials—in this case, pores with very different guest−host interaction. The largest pores of this structure have a polar surface able to have an electrostatic interaction with the CO_2 molecule which contributes to the adsorption potential. The CO_2 molecule within the small pores is practically free of that electrostatic interaction, and its interaction with the material surface is mainly through Van der Waals forces. This fact allows the filling of the largest pores through the smallest ones. A large CO_2 stabilization within the small pores would be responsible for a poor pore filling or to a very slow adsorption kinetic for CO_2 in cubic nitroprussides, which was not observed. As estimated above, CO_2 fills both the largest and the smallest pores. This is also confirmed by the estimated pore volume, which is similar from both CO_2 and H_2O adsorption (Table 3). Water is a small and polar molecule which, according to the crystal structure and the adsorption data, occupies a large fraction of the available pore volume in cubic nitroprussides.

The obtained values for the characteristic energy (E_0) (Table 3) are consistent with the discussed evidence on the guest−host interaction during the CO_2 adsorption in orthorhombic and cubic nitroprussides. The adsorption of CO_2 in the Cd^{2+} complex takes place with a large value of E_0 (14370 ± 237 J/mol), approximately two times the value obtained for this parameter in Co^{2+} nitroprusside (6929 ± 1147 J/mol), which is in accordance with the strong CO_2 interaction with the pore surface expected for the orthorhombic structure. In cubic nitroprussides, the first CO_2 molecule to be adsorbed in the largest pores also experiences a strong interaction with the polar surface. However, the following molecules to be adsorbed within the same pore experience a weaker interaction which is observed as a decrease in the resulting average adsorption energy, relative to the value found for the orthorhombic structure.

The calculated values for the adsorption potential (A) during the CO_2 adsorption in the studied materials corroborate the above-discussed results. Figure 11 shows the calculated curves for potential. As expected, the largest values of A for the CO_2 adsorption corresponds to the Cd^{2+} complex, above 18 kJ/mol at small values of the fractional adsorption θ (low relative

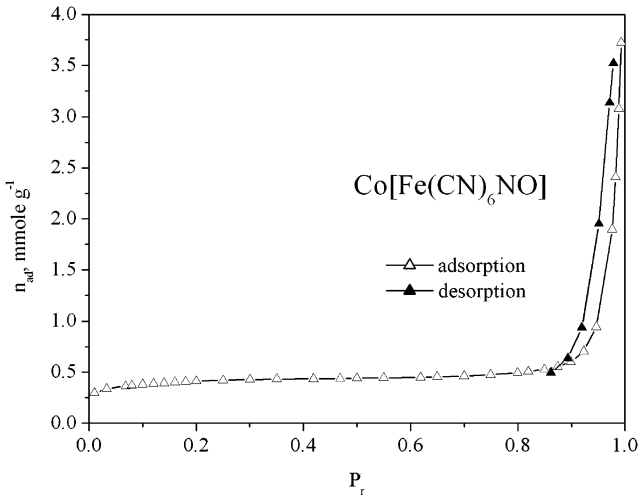

Figure 12. N_2 adsorption isotherm at −196 °C in Co^{2+} nitroprusside. According to the estimated BET area (32 m^2/g), the micropores of this material are inaccessible to N_2 at this low temperature.

pressures). The adsorption process of the first CO_2 molecules in the Co^{2+} complex is also an energetic process, with *A* values above 16 kJ/mol. As already discussed, the first CO_2 molecules to be adsorbed are involved in a strong electric field gradient−electric quadrupole moment interaction liberating a relatively large energy. Then, at higher values of θ, *A* rapidly falls due to a progressive pore filling dominated by interactions between CO_2 molecules already adsorbed and finally the filling of the small pores with a relatively weak guest−host interaction.

In the studied materials, the access to the inner pores is through relatively small windows. The nitrogen adsorption isotherms are usually recorded at −196 °C. A small cell contraction on cooling leads to a reduction in the size of these windows, which could be sufficient to hinder the access of the adsorbate (N_2) to the inner pores. In addition, at this temperature the low kinetic energy of the nitrogen molecule limits its diffusion through small windows. According to the N_2 isotherms, in the studied nitroprussides the N_2 adsorption takes place at the outer surface without filling the inner pores. Figure 12 shows the adsorption isotherm of N_2 in the Co^{2+} complex. The amount of N_2 adsorbed does not correspond to the estimated pore volume from the adsorption of water vapor and CO_2. The estimated BET area (from $P_r < 0.2$) is 32.0 ± 0.4 m^2 g^{-1}. Such a small surface area does not correspond to a microporous solid. This behavior of transition metal nitroprussides is related to the pore accessibility for the N_2 at low temperature and not to a kinetic effect due to the small window size. When the adsorption equilibrium is not reached during the adsorption experiment, the resulting isotherm shows hysteresis at low values of relative pressure, which was not observed in this case. Additional evidence of a kinetic effect results from the slope of the adsorption curve in the region of medium relative pressures. As already mentioned, a kinetic effect is usually accompanied by an adsorption curve free of saturation in that region, indicating that the adsorbed amount is determined by the chemical potential, when the diffusion through the windows is favored by a higher availability of adsorbate molecules. The adsorption isotherms of N_2 in the studied nitroprussides are free of that effect.

The nature of the observed inaccessibility of N_2 at low temperature (−196 °C) to the inner pores in nitroprussides could be related to the large polarizing power of the NO group, which deforms the environment of the iron atom in the $[Fe(CN)_5NO]$ units. The average $C_{eq}-Fe-C_{eq}$ angle (C_{eq} represents equatorial carbons) in the studied nitroprussides is 170°.[2−9] In addition, the environment of the outer metal is also distorted, on average, $N_{eq}-M-N_{eq}$ (N_{eq} represents equatorial nitrogens) is 177°.[8,9] These local distortions must be enhanced at low temperature due to a cell contraction. Probably this explains the CO_2 pore filling in these materials since in this case the adsorption experiment is carried out at 0 °C. At −196 °C, N_2 effectively fills the inner pores in ferricyanides, but with a certain kinetic effect, which suggests that in these materials the window size is close to the kinetic diameter of the nitrogen molecule (4.5 Å).[18] However, in ferricyanides the local distortions are relatively small and are mainly related to the polarizing power of the outer metal which distorts its mixed environment of cyano and aquoligands.

At the initial stage of this study, Ag^+ and Hg^+ nitroprussides were also considered. However, since their adsorption isotherms were characteristic of nonporous materials, a detailed discussion of these results was excluded from this report.

Conclusions

Stable phases of nitroprussides of divalent transition metals form a family of microporous materials with three typical crystal structures and, consequently, with three different physical behaviors. For Mn^{2+}, Fe^{2+}, Cu^{2+}, Zn^{2+}, and Cd^{2+}, the stable phases are orthorhombic (*Pnma*) dihydrates, which on dehydration lead to a microporous framework with a pore volume of about 0.111 cm^3/g. For Co^{2+} and Ni^{2+}, and also for non-aged precipitate with Fe^{2+}, the obtained material has an extended microporous structure with a pore volume above 0.360 cm^3/g. Copper nitroprusside, when obtained as precipitated samples, forms a layer structure which on heating loses the hydration water and undergoes a structural transformation to an anhydrous tetragonal phase. The small pores of this last material are inaccessible to the adsorbates used (H_2O, CO_2, and N_2). The pore systems in orthorhombic and cubic nitroprussides are accessible to water vapor and CO_2 at 23 and 0 °C, respectively, but become inaccessible to N_2 at −196 °C. This behavior is explained as related to the large polarizing power of the nitrosyl (NO) ligand which distorts the local environment of the iron atom and reduces the effective window cross section. It seems that this effect is enhanced on the cooling process until −196 °C, since CO_2, which has approximately the same kinetic diameter as N_2, shows an appropriate pore filling in an experiment carried out at 0 °C.

Acknowledgment. The authors thank Mr. J. Iglesias for his assistance in the glass equipment construction. The access to the synchrotron facilities at LNLS (Brazil) through research project 1201-2002 is gratefully recognized.

References and Notes

(1) Boxhoorn, G.; Moolhuysen, J.; Coolegem, J. P. G.; van Santen, R. A. *J. Chem. Soc., Chem. Commun.* **1985**, 1305.

(2) Mullica, D. F.; Sappenfield, E. L.; Tippin, D. B.; Leschnitzer, D. H. *Inorg. Chim. Acta* **1989**, *164*, 99.

(3) Mullica, D. F.; Tippin, D. B.; Sappenfield, E. L. *Inorg. Chim. Acta* **1990**, *174*, 129.

(4) Mullica, D. F.; Tippin, D. B.; Sappenfield, E. L. *J. Spectrosc. Crystallogr. Res.* **1991**, *21*, 81.

(5) Mullica, D. F.; Tippin, D. B.; Sappenfield, E. L. *J. Coord. Chem.* **1991**, *24*, 83.

(6) Mullica, D. F.; Tippin, D. B.; Sappenfield, E. L. *J. Coord. Chem.* **1992**, *25*, 175.

(7) Mullica, D. F.; Wardojo, T. A.; Sappenfield, E. L. *J. Solid State Chem.* **1992**, *106*, 379.

(8) Benavente, A.; de Moran, J. A.; Aymonino, P. J. *J. Chem. Crystallogr.* **1997**, *27*, 343.

(9) Gomez, A.; Reguera, E.; Cranswick, L. M. D. *Polyhedron* **2001**, *20*, 175.
(10) Gu, Z. Z.; Sato, O.; Iyoda, T.; Hashimoto, K.; Fujishima, A. *J. Phys. Chem.* **1996**, *100*, 18289.
(11) Gu, Z. Z.; Sato, O.; Iyoda, T.; Hashimoto, K.; Fujishima, A. *Chem. Mater.* **1997**, *9*, 1093.
(12) Woike, T.; Kirchner, W.; Schetter, G.; Barthel, T.; Hyungsang, K.; Haussuhl, S. *Opt. Commun.* **1994**, *106*, 6.
(13) Sato, O.; Iyoda, T.; Fujishima, A.; Hashimoto, K. *Science* **1996**, *271*, 49.
(14) Cartraud, P.; Cointot, A.; Renaud, A. *J. Chem. Soc., Faraday Trans. 1* **1981**, *77*, 1561.
(15) Harper, S. D. U.S. Patent 4,843,054 (Arco Chemical Technology Inc., Washington, DE), 1989.
(16) Kuyper, J.; Boxhoorn, G. *J. Catal.* **1987**, *105*, 163.
(17) Dunbar, K. R.; Heintz, R. A. *Prog. Inorg. Chem.* **1997**, *45*, 283.
(18) Balmaseda, J.; Reguera, E.; Gomez, A.; Diaz, B.; Autie, M. *Microporous Mesoporous Mater.* **2002**, *54*, 285.
(19) Reguera, E.; Dago, A.; Gomez, A.; Bertran, J. F. *Polyhedron* **1996**, *15*, 3139.
(20) Gomez, A. Ph.D. Thesis, Havana University, 2002.
(21) Bertran, J. F.; Reguera, E. *Solid State Ionics* **1997**, *93*, 139.
(22) Roque-Malherbe, R.; Lemes, L.; Lopez, L.; de las Pozas, C.; Montes, A. In *Natural Zeolites'93 Conference Volume*; Ming, N. W., Mumpton, P. A., Eds.; International Committee on Natural Zeolites: Brock Port, New York, 1995; pp 299−308.
(23) Dubinin, M. M. In *Progress in Surface Science and Membrane Science*; Cadenheat, D. A., Ed.; Academic Press: New York, 1975.
(24) Marquardt, D. *SIAM J. Appl. Math.* **1963**, *11*, 431−441.
(25) Stoeckli, F. *Russ. Chem. Bull., Int. Ed.* **2001**, *50*, 2265.
(26) *Active Carbon*; Bansal, R. C., Donnet, J. B., Stoeckli, F., Eds.; Marcel Dekker, Inc.: New York, 1988.
(27) Roque-Malherbe, R. *Microporous Mesoporous Mater.* **2000**, *41*, 227.
(28) Klencsar, Z. *MossWinn Program* (version 3.0, 2001); Lorand Eotvos University, Budapest 1117, Hungary.
(29) Rodriguez-Carbajal, J. *The FullProf Program*; Institute Louis Brillouin, Saclay, France, 1998.
(30) Reguera, E.; Bertran, J. F.; Miranda, J.; Dago, A. *Hyperfine Interact.* **1993**, *77*, 1.
(31) Danon, J. In *Applications of the Mössbauer Effect in Chemistry and Solid State Physics*; IAEA Publications: Vienna, 1966; p 89.
(32) Simonot-Grange, M. H. *J. Chim. Phys.* **1987**, *84*, 1161.
(33) Breck, D. W. In *Zeolites Molecular Sieves: Structure, Chemistry, and Use*; John Wiley & Sons: New York, 1974.
(34) Zhang, Y. *Inorg. Chem.* **1982**, *21*, 3886.
(35) Brown, I. D. *Acta Crystallogr.* **1976**, *A32*, 24.